Journal of Visualization, Vol. 12, No. 1 (2009) 47-55

Regular Paper

Imaging of Flame Behavior in Flickering Methane/Air Diffusion Flames

Yilmaz, N.*[1], Donaldson, A. B.*[2], Gill, W. *[2], Lucero, R. E.*[3]

*1 Department of Mechanical Engineering, New Mexico Institute of Mining and Technology, Socorro, NM 87801 USA. E-mail: yilmaznadir@yahoo.com
*2 Fire and Aerosol Sciences, Sandia National Laboratories, Albuquerque, NM 87185 USA.
*3 Department of Mechanical Engineering, New Mexico State University, Las Cruces, NM 88003 USA

Received 29 December 2007
Revised 5 July 2008

Abstract : During this study, flow visualization through the use of imaging provided visual data of the events that occurred as the flame oscillated. Imaging was performed in two different ways: 1) the first method was phase-locked imaging to capture a detailed history by simply advancing the phase angle during each image capture, 2) the second method involved high-speed imaging to gather visual image data of a natural or forced oscillating flame. For visualization, two items were considered. The first one was the shape of the flame envelope as it evolved during one oscillation cycle. From the data gathered, it was confirmed that the flame stretched in the vertical direction before quenching in the region near its center. The second consideration was imaging of the oxidizer (air) in the region immediately outside the flame. This was done by imaging the laser light reflected from particles seeded into the flow, which revealed formation of vortical structures in those regions where quenching had occurred. It was noted that quenching took place primarily by the entrainment of fresh non-reacting air into the flame. The quenching process was in turn responsible for the oscillatory behavior.

Keywords : High Speed Imaging, Air Entrainment, Flame Visualization, Diffusion Flame Oscillation.

1. Introduction

Flickering or oscillating flames are of significance in improving the understanding of turbulent combustion systems and burner pulsations have an impact on combustion equipment design. Flames oscillate periodically under certain influences such as flow rate, burner size, fuel type, and gravitational effects (Arai et al., 1999; Huang et al., 1999; Hamins et al., 1992; Sato et al., 2000; Bahadori et al., 2001; Gotoda et al., 2007; Yilmaz et al., 2007).

It is known that flame oscillation is caused by the Kelvin-Helmholtz type instability due to the buoyancy forces in the flame (Buckmaster and Peters, 1986; Katta and Roquemore, 1993; Katta et al., 1994; Azzoni et al. 1999). Diffusion flames exhibit natural oscillations of quasi-periodic frequency at the flame near the fuel source with formation of large scale vortical structures (Cetegen and Ahmed, 1993; Hamins et al., 1992).

Although there have been studies to understand natural and forced flame motions, a detailed characterization of flame oscillations is limited and not fully described due to a number of factors such as limitations of flow visualization techniques, variable flow conditions, oxidizer entrainment, chemical kinetics, turbulence, etc. Some of the previous studies include correlation of flame

frequency with flow rate, gravitational forces and other effects as mentioned above Tools used included flame luminosity (Smyth et al., 1997), temperature measurements using thin-filament pyrometry (Pitts, 1996), flame visualization using three-dimensional characterization (Bheemul et al., 2002), measurements using Planar Laser Induced Fluorescence (PLIF), Laser Doppler Velocimetry (LDV) (Lingens et al. 1996), photography and chemieluminescence from CH radicals (Hardalupas et al. 1998), Mie Scattering (Chung, 2003), and PIV (Papadopoulos et al., 2002; Fujisawa and Nakashima, 2007), imaging and diagnostics using acetone-OH simultaneous PLIF (Nakamura et al., 2008).

In this work, imaging of a methane/air diffusion flame was performed through phase-locked imaging and high-speed imaging techniques. Phase-locked imaging refers to taking an image at the same point or phase angle during every flame oscillation cycle. When viewing the imaging live, the oscillating flame appeared to be motionless and varied only slightly. With this method, it was possible to capture a detailed history for one cycle of the flow by simply advancing the phase angle during each image capture. The second technique involved high-speed imaging. When imaging at high frame rates, the same detailed visual information was achieved; only the image process was sequential in time. This method was used to gather visual image data of a naturally oscillating flame. This proved to be an equally useful method to phase locking, because the natural flame oscillations were well-defined and had little temporal and spatial variation.

For visual information, two items were considered. The first was the shape of the flame envelope as it evolved during one oscillation cycle. From the data gathered, it was confirmed that the flame stretched in the vertical direction before quenching in the region near its center. The flame stretched due to the effects of buoyancy. Once it fully quenched in the center, the flame was separated into two different parts; a small flame attached to the base of the burner and a flamelet located just above. The flamelet quenched in the center as it continued to convect upstream, then fully extinguished. This process repeated itself for both forced and unforced flames. The second consideration was imaging of the oxidizer (air) in the region immediately outside the flame envelope. This was done by imaging the laser light reflected from particles seeded into the flow. This revealed formation of vortical structures in those regions where quenching had occurred. From this, it was noted that quenching took place primarily by the entrainment of fresh non-reacting air into the flame. Entrainment was due to the vortical structures which formed as a result of roll-up of the shear layer. Therefore, it could be assumed that their existence was a result of the unstable shear layer. The quenching process was in turn responsible for the oscillatory flow.

Three primary experiments were executed, and a visual time history of the flow for three different cases was obtained:

1. Methane diffusion flame from a slot burner subjected to forced 7 Hz pulsations: flow was unseeded.
2. Methane diffusion flame from the same slot burner with no forced pulsation: flow was unseeded.
3. Methane diffusion flame from a pinhole orifice with no forced pulsation: flow was seeded.

Visualization of the unseeded flow revealed information regarding the shape of the flame envelope, whereas the seeded flow provided information regarding the flow structures that occurred on the oxidizer side. The results showed that the pulsed flow of case 1 differed significantly from the cases 2 and 3, in that the flame became detached from the burner surface. Cases 2 and 3 showed similarities for the two different burner configurations; demonstrating the same sequence of events and clearly indicating that quenching naturally occurred due to effects of air entrainment and buoyancy. In case 1, which used artificial forcing of the fuel supply, quenching was not the primary cause of the oscillations. Quenching ultimately occurred because of the forced oscillations and detachment of the flame from the burner surface. However, by forcing the flame to oscillate, a highly repeatable flow was created, and the evolution of coherent structures was easily observed.

2. Experimental Procedure

The experimental setup consisted of six different parts: (1) flame facility, (2) laser illumination, (3) CCD camera with triggering, (4) particle seeding, (5) image acquisition hardware and software, and (6) fuel supply with pulsation device. Fig. 1 is a picture of the general layout of the actual experimental arrangement used for imaging.

2.1 Case 1: 7 Hz Forcing with Phase Locking

To image the flame and investigate the flow field which resulted from forced oscillations, the flame was caused to oscillate at 7 Hz (sinusoidal) by pulsation of the fuel supply, creating a repetitive flow that resembled the natural flow except for frequency. Although the oscillations under consideration (7-10 Hz) were among the slowest driven oscillations, it was still considerably difficult to capture sequential images of the quasi-steady state and turbulent flow. Imaging with a camera, which captured frames between 30-60 Hz, yielded little or no usable information.

Therefore, to construct the complete image time history of the flame envelope oscillating at 7 Hz, the camera was phase locked to the signal of the acoustic driver used to excite the flame. This allowed for short time periods of the flow to be obtained in multiple frames. As a result, a series of highly similar images could be taken at the same time during the cycle. This time corresponded to the same phase angle in the cycle. After a series of images was acquired at a certain phase angle, data was averaged using image processing software.

For the first case (slot burner, 7 Hz forced pulsation), the fuel flow rate was 1.6 scfm (2.72 m^3/min), and the slot orifice size was 2" by 1/32" (50.8 mm by 0.794 mm). The burner was constructed from a 1/2" (21.336 mm) nominal pipe (nominal American pipe sizes do not represent true OD; true OD is provided in units of millimeters following nominal diameter), and the flame was forced to oscillate at a frequency of 7 Hz sinusoidal pulsation. The pulsation driver was set at near maximum amplitude, thus overwhelming the natural frequency of the flame. No other frequencies forced or unforced were present in the data.

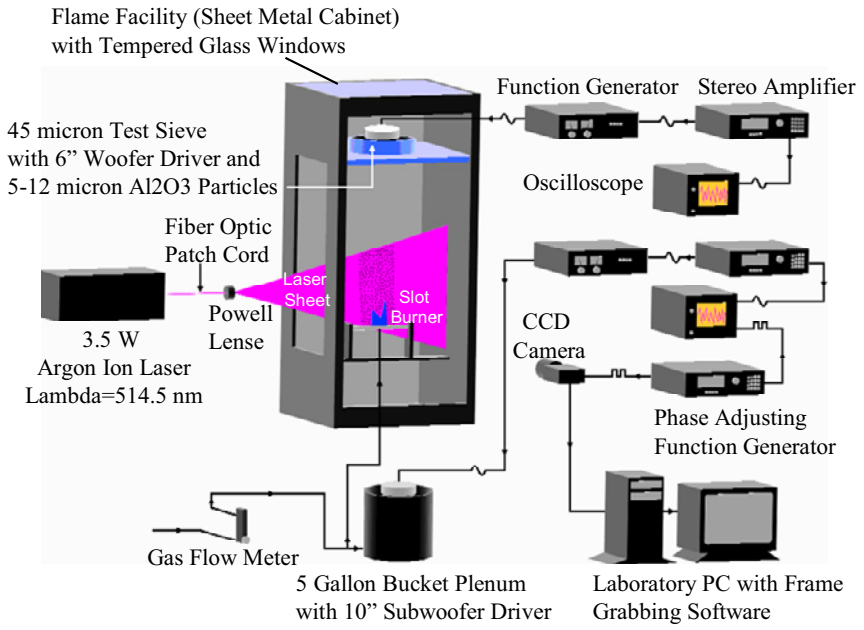

Fig. 1. Setup used to perform flame flow field visualization.

The flame was excited, using a 10" (254 mm) subwoofer chamber plumbed in the fuel supply. The subwoofer was manually pushed inside a 5-gallon plastic bucket until it created a tight seal, forming a chamber to store low-pressure (approximately 0.3 psig-or 2.068 kPa) methane gas. The gas inside was pulsed by the speaker. The subwoofer was driven at controlled frequencies and amplitudes, using an arbitrary waveform generator and audio power amplifier. As mentioned before, the excitation waveforms were sinusoidal. The amplitude on the waveform generator was kept at 20 V. The flame, which was fed methane at the specified flow rate, was forced to oscillate at the maximum amplitude possible without extinguishing the flame. The driving voltage of the power amplifier was adjusted by fine- and coarse-adjusting potentiometers, which were monitored using a data acquisition system, that measured and recorded the RMS and mean voltage across the electrical terminals of the subwoofer.

Once the flame was set to oscillate at this frequency, a 7 Hz signal of TTL level was used to synchronize the camera trigger to the pulsation of the flame, thus placing the camera trigger directly in phase with the flame pulsation. With both the flame and camera trigger in phase with each other, a first set of images was taken. After the first set of images was acquired, the phase angle of the TTL signal that drove the camera trigger was advanced by five degrees. The procedure was repeated until image sets for a full 7 Hz cycle were captured.

Images were taken at each phase angle in order to construct a flow history of one 7 Hz pulse cycle. The phase angle between images was five degrees for a total of 72 images for the cycle. Ten images were captured at each phase angle to ensure no large variances. When placed in sequential order according to phase, the time between images, as though they were captured sequentially in time, was on the order of 2 ms. A visual time history of the flow was constructed by averaging the 10 images of each sequence at every angle. This was done to get basic visual information of the pulsed flow. When these images were placed in order of increasing angle, a visual time history of the flow for one cycle was seen and the events that occurred during one cycle of the developing flow became very clear.

2.2 Cases 2 and 3: No Forcing with Phase Lag

Case 2 involved imaging of a naturally oscillating methane diffusion flame. The burner size and the flow rate were kept the same as in case 1. In addition, the imaging method was slightly different. Instead of phasing locking to the natural oscillation frequency of the flame, the camera was triggered to image at a slightly lower frequency. The oscillation frequency of the flame was well-defined and had little time variation. However, frequency was not measured and remained unknown during this experiment.

Despite the unknown flame frequency, the frequency of the camera trigger was carefully adjusted and set to occur at a frequency slightly lower than that of the oscillating flame. This created a small amount of phase lag between the camera trigger and the oscillating flame, on the order of several tenths of a Hertz. Imaging in this way allowed for the flame oscillation cycle to be significantly slowed, thus allowing for the events occurring in the plume to be imaged with great detail.

The same procedure was used in case 3, which involved imaging of a naturally oscillating flame from a 1/4" (13.716 mm) nominal diameter pipe burner with centerline oriented horizontally with 1/16" (1.5875 mm) pinhole orifice in the side instead of the slot burner. In this experiment, the volume field around the burner assembly was uniformly seeded with 5-12 micron aluminum oxide particles. The laser light scattered from the particles was imaged using a CCD camera. In addition to the light, the radiation of the luminous plume was also imaged as in case 1. The seeding of the field allowed for the image capture of the coherent structures present immediately outside the flame envelope.

3. Results and Discussion

3.1 Case 1: Flame Envelope History of Methane Diffusion Flame, (Slot Burner, 7 Hz Forcing, Unseeded)

Images of the flame structures at progressive sequence for one 7 Hz cycle are shown in Fig. 2. These images are only 12 of the 72 total averaged images, and were captured using the procedure described previously. The phase angle between the images shown in the figure is 30 degrees. For this case, the flow was not seeded. Therefore, the image set served only as basic visual representation of the evolvement of the flame.

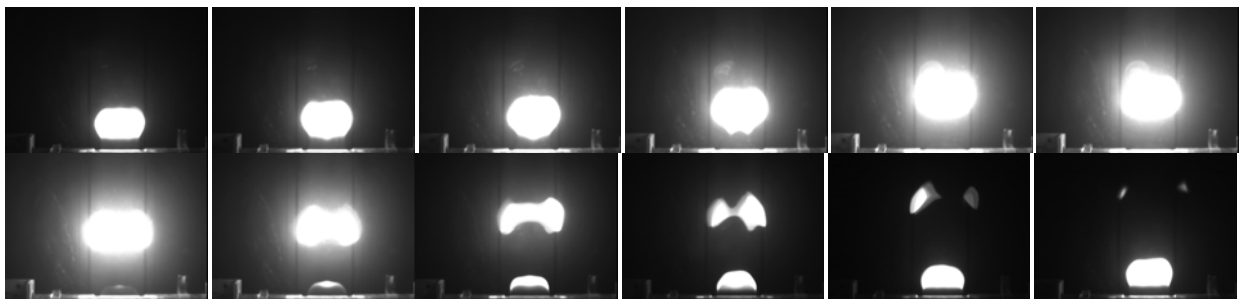

Fig. 2. Phase locked images for a methane diffusion flame from a slot burner which was forced at 7Hz.

During this experiment the flame was forced to oscillate using the subwoofer. The positive displacement of the subwoofer driver increased the local velocity of the flame envelope during various points of the pulse cycle. At these distinct points, the buoyant reaction zone became rich with fuel, and the flame bulged until it almost formed a circle. In Fig. 2, it is evident that the jet diffusion flame was sensitive to pulsing of the fuel stream.

In addition, during this time interval, the enlarged flame front translated in the vertical direction, as shown in Fig. 2. These findings were in much agreement with available data in the literature (Chen et al., 1993), where a similar increase in the local width of the luminous plume was observed. Once the positive displacement of the subwoofer driver began to end, it began a negative displacement and therefore caused the reacting jet to experience a severe decrease in velocity.

Once the driver reached the bottom of its stroke during the 7 Hz cycle, the velocity of the flame was momentarily paused. As a result of this, the bulged flame envelope became detached from the burner surface and continued to translate in the vertical direction. This happened due to the flame's initial velocity and the effect of buoyancy. Therefore, no flame existed at the base of the burner. As the flame continued to move in the vertical direction, it separated into two axisymmetric flamelets, which also convected and distorted under the influence of buoyancy. Re-ignition of fuel at the burner orifice is seen to occur in the 8th of 12 images. The mechanism for ignition is unknown but can be speculated to be caused by: 1) radiation from the detached flamelet, 2) from unseen radical species remaining in the neighborhood of the burner orifice, or 3) from elevated temperature of the pipe. Identification of the precise cause could make an interesting and informative investigation.

In addition, this is the point during the cycle when the axisymmetric vortices surrounding the flame met and quenched the flame at its center. Fresh air entrainment, which is presumed responsible for quenching the flame, is a direct result of vortical formation. It was also reported that high local strains produced by vortical motion were observed in the region where extinction (quenching) occurred (Chen et al., 1993).

3.2 Case 2: Flame Quenching and Extinction (Slot Burner, No Forcing, Unseeded)

The main advantage of triggering with a digital waveform generator was the ability to fine tune the frequency of the output signal. With accuracy up to 0.01 Hz, the frequency of the output signal was tuned to closely match the frequency at which the flame oscillated. Since the frequency at which the flame naturally oscillated was well-defined and varied very little with time, the digital camera was triggered to capture images of the developing flow within a few degrees of phase lag. The result was a detailed time history of the flow for one cycle. Some images were captured using this approach, and some findings were made.

The images in Fig. 3 clearly demonstrate the bulging, stretching, necking, separation, and extinction of the propagating flame front. From the images, two vortical structures may have begun to form on each side of the flame near the base of the burner. They may have been caused by the shear layer which exists between the flame envelope and the surrounding air. Immediately after, the entrainment of air into the flame occurred. These structures appeared to react with the flame jet due to the distortion of the flame itself. As the cycle progressed, the size of the vortical structures increased in size as their centers translated in the vertical direction. As a result, the flame also stretched and began to neck in the vertical direction, while simultaneously becoming thinner. While

the flame continued necking, the vortical structures become even larger in size as they translated upward. From the images, it is evident that they became large enough in radius and forced the flame to separate into two flamelets; one remained attached to the burner and the other lifted off, separated and then burned out.

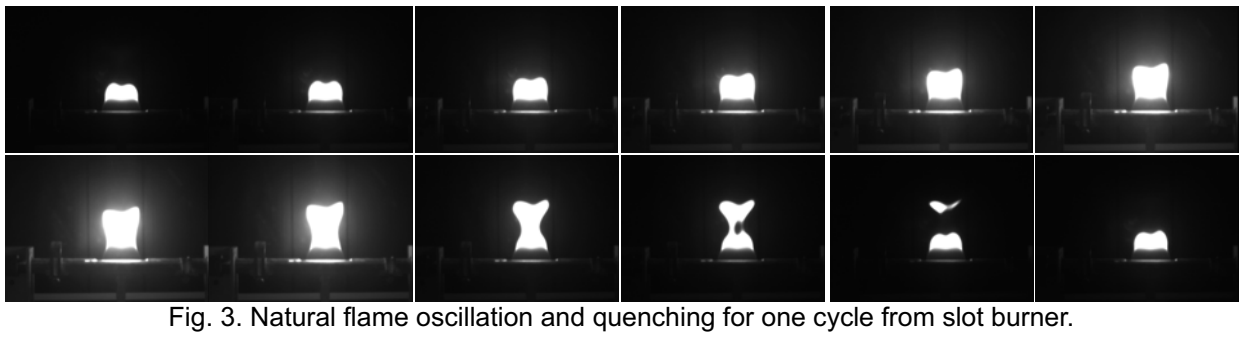

Fig. 3. Natural flame oscillation and quenching for one cycle from slot burner.

One striking difference between the actual flow and the pulsed flow investigated in the previous section was that a flame existed at the base of the burner throughout the entire cycle during natural oscillation. This is a strong indication that the large-scale vortical structures began small at the base of the burner due to the roll-up of the unstable shear layer. Once vortical formation occurred, air entrainment followed; promoting the acceleration of the flame front in the vertical direction. As entrainment continued, the structures became larger and translated in the vertical direction. They did this until the air entrainment became great enough to quench the flame, presumably when the lean flammability limit was reached.

3.3 Case 3: Flame Quenching and Extinction (Pinhole Orifice, No Forcing, Aluminum Oxide Seeded Flow)

In the final imaging experiment, the burner was constructed from a horizontal 9" (228.6 mm) long 1/4" (13.716) nominal diameter steel pipe with a 1/16" (1.5875 mm) pinhole orifice at the middle position on one side of the pipe. The flow rate of the methane fuel remained the same at 1.6 scfm (2.72 m^3/min); this was chosen to assure that the natural oscillation of the flame was strong and well defined. Also, the test volume was uniformly seeded with 5-12 micrometer particles of aluminum oxide powder, so that laser light scattered from the particles could be imaged and allow visualization in the oxidizer (air) region. Melling (1997) provided guidance on relationship between the turbulent frequencies and response of particles in a flame, and using formulae provided, an alumina particle of mean size 8.5 microns should respond to frequencies of up to 84 Hz, which is above the frequencies of interest in this study, i.e., on order of 7-12 Hz for the methane diffusion flame at available fuel flow rates. The same phase lag imaging method used in case 2 was used in this experiment.

As shown in Fig. 4, it is evident that the flame was not oscillating, but rather transitioning through a series of different events. As mentioned previously, these involved stretching, necking, and finally quenching. All three events occurred during one cycle of oscillation. The frequency of this sequence of events was largely,-and probably ultimately, controlled by the rate at which vortical structures formed and convected upward. As a result, air entrainment occurred and the flame quenched.

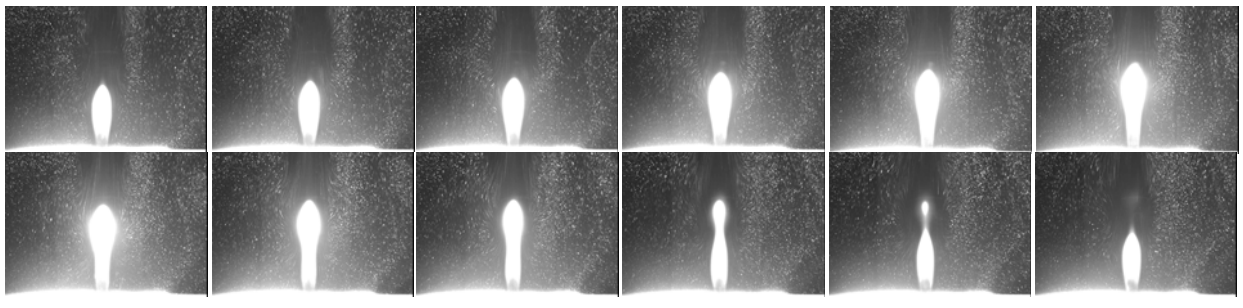

Fig. 4. One cycle for a pinhole burner with seeding and without forcing, showing quenching of flame.

The frequency of oscillation is proportional to the jet exit velocity (Gutmark et al., 1990) and at high flow rates, the vortical structures on opposing sides of the jet became offset from each other due flow instability. Therefore, quenching did not occur. Quenching was most likely to occur when the size of the opposing structures became large enough that the outermost air entrainment on each structure simultaneously met at the core of the jet. At this point, enough cool ambient air had entered the reaction region at a sufficiently large transverse velocity to quench the flame near the upper height limit of the flame. This occurred in a somewhat pinching fashion. It should be noted that the velocity of the jet in this region became low enough in the vertical direction that it was dominated by the rush of ambient air entering the flame in the horizontal direction. The entire process began with the entrainment of air into the reaction zone due to the initial roll-up of the unstable shear layer just above the surface of the burner.

A cross-section of the flow shows the movement of air into the reaction region near the base of the flame at the pinhole orifice. The velocity of the air was large enough to create an initial shear layer disturbance. The air in this region entrained horizontally until the jet directed it upward. While being directed upward, the jet added rotational velocity to the air, causing circulation. At this point, the flow became rotational, setting the stage for vortical formation. As the process is shown in Fig. 5, it can easily be noticed in the figure that the shape of the flame jet is heavily influenced by the vortices formed in the surrounding (ambient) air. The arrowheads near the burner indicate air entrainment induced by the onset of mixing between fuel and air causing a roll-up of the shear layer. The circles indicate vortex formations. As mixing and air entrainment increase, the effects of buoyancy begin to heavily dominate the flow.

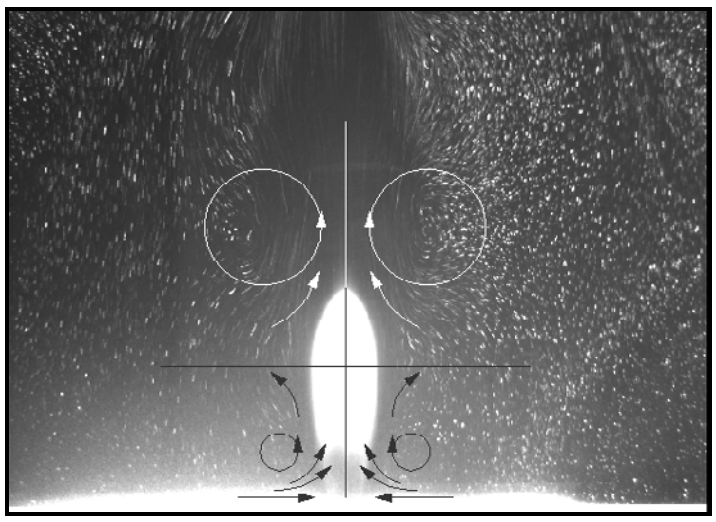

Fig. 5. Various flow paths and structures of the buoyancy driven oscillating flame front from pinhole orifice. Flow seeded with 5-12 micron alumina.

When closely examined, the vortical structures did not appear to be circular in shape. Instead they appeared to be elliptical in shape close to the centers. From further distances, the structures appeared to form a saddle-like shape. This was caused by two processes: the steep velocity gradient which existed between the ambient air and the jet, and air's low resistance to shear. Viewing the image, it can be proposed that the oscillating flow was initially and primarily caused by the air entrainment. Air entrainment was a subsequent result of vortical formation. In Fig.5, a horizontal line divides the air that is influenced by buoyancy and vortical structures downstream and the air that is influenced by entrainment upstream near the burner surface. When further examined, it can be seen that the structures become strong enough to quench the flame at a certain height. This can be seen in Fig.6. This image was taken near the end of a 7 Hz cycle. The burner used to generate the flame in Fig.6 was the slot burner. In this case, the flow was seeded with 5-12 micron diameter aluminum oxide particles. The vortex roll-up is shown near the base of the flame. The arrowheads indicate the flow of air as it was entrained into the flame. The image shows strong spiral formation. Spiral nodes are located just below the flamelets.

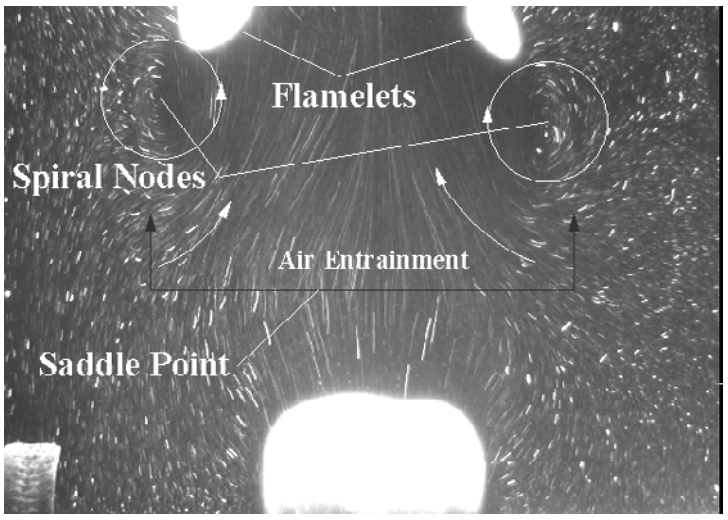

Fig. 6. Various flow paths and structures of the 7 Hz driven oscillating flame from the slot burner. Flow seeded with 5-12 micron alumina.

4. Conclusion

Imaging was employed to visually investigate the quasi-steady nature of the flickering flame. It was determined from the captured images that the flame was not oscillating between two positions, as initially suspected. Instead, the flame was quenching in the center below the flame height. It was found that this could have been due to reaction-induced air entrainment near the base of the burner where mixing initially occurred causing a disturbance in the shear layer. The unstable shear layer then rolled up, creating buoyancy induced vortical formation and subsequent fresh air entrainment. This could be true for both the pulsed and non-pulsed flame.

The shape of the flame envelope of the pulsed flame differed greatly from that of the non-pulsed flame. From the images acquired for the case of the pulsed flame, it was found that the flame quenched at the base of the burner, thus causing it to completely detach itself from the burner surface and convect upward thus allowing entrainment of fresh air. As it moved in the vertical direction, its shape was distorted due to the effects of buoyancy and vortical formation. Finally, the lifted flame separated into two smaller flamelets and then entirely quenched.

This was certainly not the case with the naturally oscillating flame. Instead, the natural oscillations (possibly resulting from air entrainment and vortical formation) caused the flame to stretch, neck, and finally quench. The naturally oscillating flame was similar to the pulsed flame, in that it quenched in the center near the flame height and then separated into two smaller flamelets, which later distorted and quenched due to buoyancy and cool air. However, it should be noted that, throughout the entire cycle, the flame remained attached to the burner. Therefore, it can be concluded that the pulsed flame did not entirely resemble the naturally oscillating flame.

References

Arai, M., Sato, H., Amagai, K. (1999). Gravity effects on stability and flickering motion of diffusion flames. Combustion and Flame, 118(1-2), 293-300.

Azzoni, R., Ratti, S., Puri, I. K., Aggarwal, S. K. (1999). Gravity effects on triple flames: Flame structure and flow instability, Physics of Fluids, 11(11), 3449-3464.

Bahadori, M. Y., Zhou, L., Stocker, D. P., Hegde, U. (2001). Functional dependence of flame flicker on gravitational level. AIAA Journal, 39(7), 1404-1406.

Bheemul, H.C., Lu, G., Yan, Y. (2002). Three-dimensional visualization and quantitative characterization of gaseous flames. Measurement Science and Technology, 13(10), 1643-1650.

Buckmaster, J., Peters, N. (1986). The infinite candle and its stability: a paragism for flickering diffusion flames. 21st Symposium (International) on Combustion, the Combustion Institute (Pittsburg), 1829-1836.

Cetegen, B. M., Ahmed, T. A. (1993). Experiments on the periodic instability of buoyant plumes and pool fires. Combustion and Flame, 93(1-2), 157-184.

Chen, T. Y., Hedge, U. G., Daniel, B. R., Zinn, B. T. (1993). Flame radiation and acoustic intensity measurements in

acoustically excited diffusion flames. Journal of Propulsion and Power, 9(2), 210-216.
Chung, S. H. (2003) Several applications of laser diagnostics for visualization of combustion phenomena. Journal of Visualization, 6(2), 95-106.
Fujisawa, N., Nakashima, K. (2007). Simultaneous measurement of three-dimensional flame contour and velocity field for characterizing the flickering motion of a dilute hydrogen flame, Measurement Science and Technology, 18(7), 2103-2110.
Gotoda, H., Ueda, T., Shepherd, I. G., Cheng, R.K. (2007). Flame flickering frequency on a rotating Bunsen burner. Chemical Engineering Science, 62(6), 1753-1759.
Gutmark, E., Parr, T. P., Hanson-Parr, D. M., & Schadow, K. C. (1990). Coherent and random structure in reacting jets. Experiments in Fluids, 10(2-3), 147-156.
Hamins, A., Yang, J. C., Kashiwagi, T. (1992). Experimental investigation of the pulsation frequency of flames. Symposium (International) on Combustion, 1695-1702.
Hardalupas, Y., Selbach, A., Whitelaw, J. H. (1998). Aspects of oscillating flames. Journal of Visualization, 1(1), 79-86.
Huang, Y., Yan, Y., Lu, G., Reed, A. (1999). On-line flicker measurement of gaseous flames by image processing and spectral analysis. Measurement Science and Technology, 10(8), 726-733.
Katta, V. R., Roquemore W. M. (1993). Role of inner and outer structures in transitional jet diffusion flame. Combustion and Flame, 92(3), 274-282.
Katta, V. R., Goss, L. P., Roquemore W. M. (1994). Effect of nonunity Lewis numbers and finite-rate chemistry on the dynamics of a hydrogen-air jet diffusion flame, Combustion and Flame, 96(1-2), 60-74.
Lingens, A., Reeker, M., Schreiber, M. (1996). Instability of buoyant diffusion flames, Experiments in Fluids, 20(4), 241-248.
Melling, A. (1997). Tracer particles and seeding for particle image velocimetry, Measurement Science and Technology, 1406-1416.
Nakamura, Y., Manome, S., Yamashita, H. (2008). Imaging and diagnostics of turbulent methane-air premixed flames by acetone-OH simultaneous PLIF.
Papadopoulos, G., Bryant, R. A., Pitts, W. M. (2002). Flow Characterization of flickering methane/air diffusion flames using particle image velocimetry, Experiments in Fluids, 33(3), 472-481.
Pitts, W. M. (1996). Thin-filament pyrometry in flickering laminar diffusion flames. Symposium (International) on Combustion, 1, 1171-1179.
Sato, H., Amagai, K., Arai, M. (2000). Diffusion flames and their flickering motions related with Froude numbers under various gravity levels. Combustion and Flame, 123(1), 107-118.
Smyth, K. C., Harrington, J. E., Johnsson, E. L., Pitts, W. M. (1993). Greatly enhanced soot scattering in flickering CH4/air diffusion flames. Combustion and Flame, 95(1-2), 229-239.

Author Profile

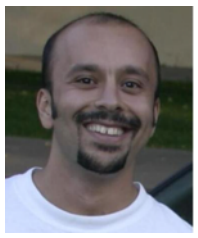

Nadir Yilmaz: Dr. Yilmaz received his Bachelor of Science in Mechanical Engineering from Istanbul Technical University in 1999, Master of Science in Mechanical Engineering from Bradley University in 2001 and Ph.D. in Mechanical Engineering fro m New Mexico State University in 2005. After obtaining his Ph.D., he worked as an assistant professor at New Mexico State University until 2006. He works as an assistant professor in Mechanical Engineering at New Mexico Institute of Mining and Technology since 2006. His research interests are computational fluid dynamics, combustion, chemical kinetics, alternative fuels and internal combustion engines.

A. Burl Donaldson: Dr. Donaldson received a MS degree in Chemical Engineering from the University of Utah in 1965 and PhD in Mechanical Engineering from New Mexico State University in 1969, where he teaches now. He worked at Sandia National Laboratories-Albuquerque for 12 years, and with a venture company seeking to commercialize direct contact steam generators for heavy oil recovery for 8 years. He maintains part time employment at Sandia with an emphasis on heat transfer in solid and liquid rocket propellant fires, but also works with IC and EC engines with a focus on emissions and alternate fuels.

Walter Gill: Dr. Gill received his Bachelor of Science in 1969, Master of Science in 1971 and Ph.D. in 1979, in Mechanical Engineering from New Mexico State University. Dr. Gill has served in several technical positions including his current position as a Member of Senior Staff at Sandia National Laboratories where he is involved in various thermal measurements; principally with measurements and characterization of the thermal environments in fires. Specific environments of interest are large hydrocarbon pool fires and solid propellant fires.

Ralph E. Lucero: He received his Bachelor of Science in Mechanical Engineering from New Mexico State University in 2004, Master of Science in Mechanical Engineering from New Mexico State University in 2006. His areas of expertise are experimental combustion, particle image velocimetry and thermal sciences.